Indian Journal of Chemistry
Vol. 63, September 2024, pp. 847-854
DOI: 10.56042/ijc.v63i9.8369

A molecular hybridization approach to design and study the *in vitro* and *in silico* properties of N-phenyl-4-oxo-butanamide derivatives

Sruthi Sri Bothsa, Hymavathi Veeravarapu, Sangeetha Guruvelli, Shobha Singarapalle, Tulasi Prasanthi & Murali Krishna Kumar Muthyala*

Pharmaceutical Chemistry Research Lab, AU College of Pharmaceutical Sciences,Andhra University, Visakhapatnam 530 003, India
E-mail: profmmkau@gmail.com, dr.mmkkumar@andhrauniversity.edu.in

Received 29 January 2024; accepted(revised) 28 June 2024

In the present study, a molecular hybridization approach has been used to design and synthesise N-phenyl-4-oxo-butanamide derivatives as potent anti-TB agents. A total of 28 target compounds have been synthesized. Among the tested compounds, **4c**: N-(2,4-difluorophenyl)-4-oxo-4-(4-phenylpiperazin-1-yl) butanamide and **4d**: N-(2,4-difluorophenyl)-4-oxo-4-(4-benzylpiperazin-1-yl) butanamide, have been identified as potent anti-TB agents with an MIC = 1.56 µg/mL against *M. tuberculosis* H37Rv. Interestingly, these compounds do not show appreciable antibacterial and no antifungal activity, clearly indicating their selectivity towards *M. tuberculosis.* Docking simulation on enzymes involved in mycolic acid biosynthesis result in the identification of InhA as the putative enzyme target for these compounds. The compounds **4c** and **4d** show the highest binding affinity, below –10.0 kcal/mol.

Keywords: *Mycobacterium tuberculosis*, 2-Transenoyl-acyl carrier protein (ACP), Reductase (InhA), N-phenyl-4-oxo-butanamide derivatives, MABA assay, Molecular docking

Tuberculosis, an infectious disease attributed to *Mycobacterium tuberculosis* (Mtb), primarily targets the pulmonary system[1]. It is an air born, highly contagious disease. Uniqueness of *M. tuberculosis* is the thick cell envelope with an outer membrane primarily composed of long-chain mycolic acids (MA)[2,3]. These lipids are crucial for the bacteria's viability and/or resistance[4-6]. Much is known about the pathways responsible for MA synthesis, which is centered on two fatty acid synthase activities: FAS-I and FAS-II (Fig. 1). They are responsible for the formation of 16 to 24 carbon length fatty acids that are elongated to form long chain high molecular mass mycolates[7-11]. Mycolate biosynthesis is the main target of several front-line therapies used for treating mycobacterial infections. The enzymes in the unusual type II fatty-acid synthase involved in this process represent attractive targets for drug development[12-16]. The key enzymes involved in mycolic acid biosynthesis are 2-transenoyl-acyl carrier protein (ACP) reductase (InhA)[17], β-ketoacyl ACP synthase I (KasA)[18], mycolic acid methyl transferases (MmaA1)[19], β-Ketoacyl-Acyl Carrier Protein Reductase (MabA)[20] and Beta-Ketoacyl-Acyl Carrier Protein Synthase III (FabH) [21]. Their complete study and 3D structures are available, making structure based drug design a possibility.

Our research group has been working on discovery of potent anti-TB lead molecules. We recently reported anti-TB activity of 1,4-diketo compounds[22] and N-substituted glycinamide derivatives[23] both have shown high affinity towards enzymes involved in mycolic acid biosynthesis. Inspired by this discovery of anti-tubercular properties of these two scaffolds, we employed a molecular hybridization approach to unlock the potential synergies within these motifs. Our hypothesis was that combining these scaffolds resulted in the formation of N-phenyl-4-oxo-butanamide derivatives or Succinimides (Fig. 2), born from this strategy, could exhibit enhanced anti-tubercular activity compared to their individual components. Using this design strategy, as depicted in Scheme 1, a series of 28 compounds were synthesized and tested for their *in vitro* anti-TB activity against *M. tuberculosis* H37Rv strains using the Microplate Alamar Blue Assay (MABA), and deduced their structure-activity relationship. We also performed molecular docking studies of the synthesized compounds on selected proteins that are involved in the cell wall synthesis of *M. tuberculosis*.

Experimental Work

Materials and Methods

The synthesis procedure utilized solvents and chemicals from commercial sources without further

purification. All reactions were monitored using an appropriate mobile phase by analytical thin-layer chromatography (TLC) on Merck DC plates (aluminum-based silica gel 60 F254) purchased from Merck KGaA. The spots were visualized using UV (254 nm), iodine, and acid spray, respectively. The melting points were measured on a Digimelt melting point apparatus (Stanford Research Systems, USA) and were uncorrected. ^{1}H NMR and ^{13}C NMR spectra were acquired from the Bruker system (400 MHz for ^{1}H and 100 MHz for ^{13}C). $CDCl_3$ and DMSO-d6 were used as NMR solvents and tetramethylsilane (TMS) as an internal reference. Chemical shift values were expressed in parts per million (ppm), and coupling constant values in hertz (Hz) using the following multiplicity abbreviations: singlet (s), doublet (d), triplet (t), and multiplet (m). For elemental analysis experiments, a Carlo Erba elemental analyzer was utilized. The Thermo Scientific Orbitrap Exploris 120 MS system was utilized for ESI-MS mass spectral studies. FTIR spectra were recorded with Bruker (ALPHA-T) FTIR spectrometer using KBr pellet method or ATR ZnSe method as applicable. The IR data was processed by Opus 7.0 software.

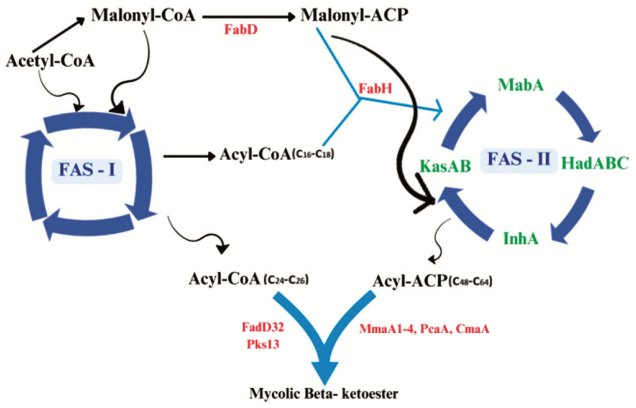

Fig. 1 — Overview of Mycolate biosynthesis pathway

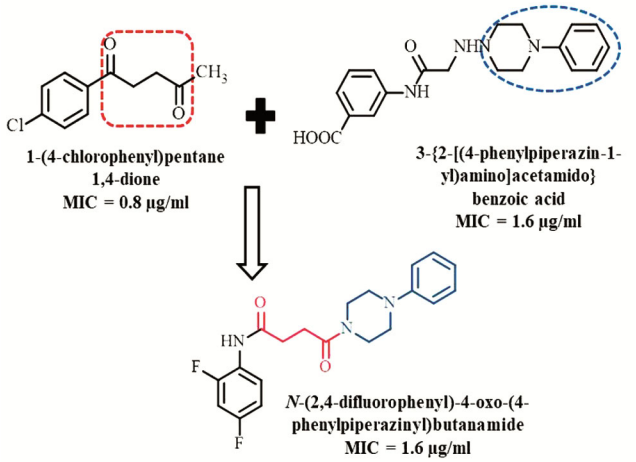

Fig. 2 — Designed strategy for the synthesis of Succinimide derivatives

Chemistry

Step-1) General procedure for the synthesis of substituted succinamic acid[24-26]

10mmol of succinic anhydride was weighed out and placed in a dry RBF with a magnetic stir bar. Dried THF (30 mL) was added and stirred to dissolve the succinic anhydride. Add Aromatic amines (10mmol) dropwise to the solution and allow the reaction mixture to reflux for 3 hours. After completion of reaction as indicated by TLC, quench the reaction using ice cold water. Chilled hexane (30 mL) was added to the cold reaction flask to precipitate the corresponding succinamic acid. The product was collected by suction filtration using a Buchner funnel and then rinsed with 20 mL of hexane. Precipitate was collected, recrystallized, and dried. The obtained precipitate was used for the next reaction without any further purification.

Step-2) General procedure for the synthesis of *N*-phenyl-4-oxo-butanamide derivatives[27]

The synthesis of the title compounds **1a-g**, **2a-g**, **3a-g**, **4a-g** involves an acid-amine coupling reaction. In a round-bottom flask (RBF), 500 mg of the corresponding succinamic acid (2.181 mmol, 0.65 eq)

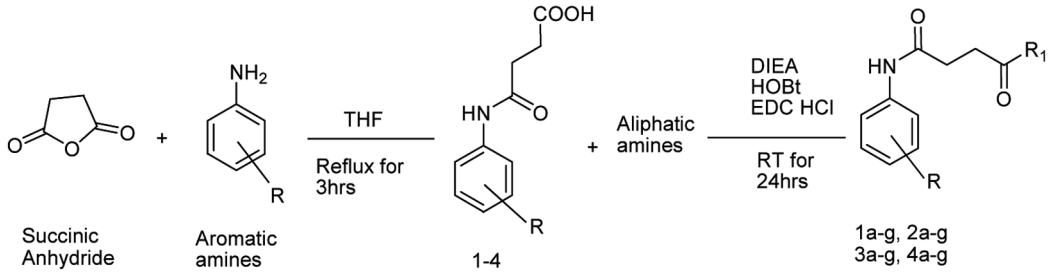

Scheme 1 — Synthesis scheme for N-phenyl-4-oxo-butanamide derivatives

was placed, and 2 mL of DMF was added, followed by stirring. To this 1.15 mL DIEA (6.609mmol, 1.97 eq) was added and cooled to 0°C, kept stirring for 5 minutes. Subsequently, 849 mg EDC HCl (4.42 mmol, 1.32 eq), 678 mg HOBt (4.42 mmol, 1.32 eq), and aliphatic amine (3.35 mmol, 1 eq) were added and stirred at RT for 24 hours. After completion of the reaction, as indicated by TLC, the reaction mixture was poured onto ice-cold water, and the precipitate obtained was filtered through vacuum filtration followed by recrystallization with methanol to get a pure compound.

Characterization of potent compounds (the Supplementary Information section presents the data for the remaining compounds)

***N*-(2,4-Difluorophenyl)-4-oxo-4-(4-phenylpiperazin-1-yl) butanamide**, **4c**: Yield 75.4%. m.p.125-128°C. IR (KBr): 1625 (C=O), 1729 (C=O), 3260 (Ar C-H), 3272 (NH) cm^{-1}; ^{1}H NMR (400 MHz, $CDCl_3$): δ 8.42 (1H, m, Ar-H), 8.21 (1H, m, Ar-H), 7.29 (1H, m, Ar-H), 6.94 (3H, m, Ar-H), 6.84 (2H, m, Ar-H), 3.69 (4H, m, CH_2), 3.18 (4H, m, CH_2), 2.82 (2H, t, CH_2), 2.81 (2H, t, CH_2); ^{13}C NMR (100 MHz, $CDCl_3$): δ 170.99 (Aryl C(=O)NH), 170.33 (Aryl C(=O)NH), 164.96 (Ar-C), 161.08 (Ar-C), 150.85 (Ar-C), 129.28 (CH), 123.07 (CH), 120.64 (CH), 116.69 (Ar-C), 111.10 (CH), 110.85 (CH), 103.78 (CH), 49.59 (CH_2), 45.32 (CH_2), 30.93 (CH_2), 28.74 (CH_2); HRMS (ESI): *m/z* Calcd for $C_{20}H_{21}F_2N_3O_2$: $[M+H]^+$: 374.16. Found: 374.16. Anal. Calcd for $C_{20}H_{21}F_2N_3O_2$: C, 64.33; H, 5.67; F, 10.18; N, 11.25; O, 8.57. Found: C, 64.32; H, 5.66; F, 10.17; N, 11.24; O, 8.56%.

***N*-(2,4-Difluorophenyl)-4-oxo-4-(4-benzylpiperazin-1-yl) butanamide**, **4d**: Yield 71.8%. m.p.149-151°C. IR (KBr): 1642 (C=O), 1683 (C=O), 3215 (Ar C-H), 3274 (NH) cm^{-1}; ^{1}H NMR (400 MHz, $CDCl_3$): δ 8.48 (1H,m, Ar-H), 8.20 (1H, m, Ar-H), 7.79 (1H, m, Ar-H), 7.62 (1H, m, Ar-H), 7.28 (2H, m, Ar-H), 6.83 (2H, m, Ar-H), 3.66 (2H, m,CH_2), 3.54 (4H, m,CH_2), 2.75 (2H, t, CH_2), 2.74(2H,t,CH_2) 2.45 (4H, m,CH_2); ^{13}C NMR (100 MHz, $CDCl_3$): δ 173.11 (Aryl C(=O)NH), 170.17 (Aryl C(=O)NH), 168.8 (Ar-C), 159.73 (Ar-C), 136.10 (Ar-C), 128.37 (CH), 127.36 (CH), 125.05 (CH), 124.14 (Ar-C), 118.53 (CH), 110.11(CH), 104.61 (CH), 62.82 (CH_2), 52.63 (CH_2), 45.34 (CH_2), 32.58 (CH_2), 28.86 (CH_2); HRMS (ESI): *m/z* Calcd for $C_{21}H_{23}F_2N_3O_2$: $[M+H]^+$: 388.18. Found: 388.18. Anal. Calcd for $C_{21}H_{23}F_2N_3O_2$: C, 65.10; H, 5.98; F, 9.81; N, 10.85; O,8.26. Found: C, 65.09; H, 5.97; F, 9.80; N, 10.84; O, 8.25%.

Anti-tubercular activity

Microplate Alamar Blue Assay (MABA)[28-30] is a rapid, high-throughput, inexpensive dye-based cell viability assay which uses Alamar blue as an indicator for anti-mycobacterial drug screening. MABA helps in quantitative determination of drug susceptibility of replicating *Mycobacterium tuberculosis* H37Rv (ATCC 27294). The synthesized compounds were evaluated for their *in vitro* anti-tubercular activity against H37Rv strain using MABA assay, and the activity is given as minimum inhibitory concentration (MIC) in μg/mL. The results are presented in Fig. 4 and Table 2.

Anti-microbial activity

The agar well diffusion method[31] was used to test the bacterial susceptibility of the synthesized compounds at various concentrations. Using Rifampicin as the standard and DMSO as the control, antibacterial activity against *Staphylococcus aureus* (ATCC 25923) and *Escherichia coli* (ATCC 26) was tested. Ketoconazole was used as the standard and DMSO as acontrol for testing antifungal activity against *Candida albicans* (ATCC 10231). At a concentration of 100 μg/mL, none of the synthesized compounds exhibited appreciable antimicrobial activity against the selected strains.

Molecular docking Studies

The structures of compounds **1a-g**, **2a-g**, **3a-g**, **4a-g** were drawn using Chem Draw 19.0, and Chem3D was used to optimize ligand geometry and perform MM2 energy minimization of the 3D structures.[32] 2-transenoyl-acyl carrier protein (ACP) reductase(InhA), β-ketoacyl-ACP reductase (MabA), beta-ketoacyl-acyl carrier protein synthase III (FabH) and β-ketoacylACP synthase I (KasA) protein X-ray crystal structures were obtained from (www.rcsb.org/pdb/home/home.do) and mycolic acid methyl transferase (MmaA1) protein is a homology model developed in our lab from a previous study.[19] Charges were assigned for the protein and the ligand using AutoDockTools (ADT). Receptor site was also defined *via* GRID box parameters using ADT.[33] The docking experiment was carried out using the molecular docking tool Vina (version 1.1.2)[34] using AUDockerLE interface. The receptor-ligand

interactions were analysed using Discovery Studio Visualizer[8] v21.1.0.20298.[35]

Results and Discussion

The N-phenyl-4-oxo-butanamide derivatives **1a-g**, **2a-g**, **3a-g**, **4a-g** were obtained *via* a two-step straight forward reaction (Scheme 1). In the first step, succinic anhydride is made to react with aromatic amines to obtain the intermediates, succinamic acids. The resulting intermediates, *i.e.*, succinamic acids are then reacted with aliphatic amines (given in Table 1) to yield a total of 28 novel N-phenyl-4-oxo-butanamide derivatives.

The chemical structures of the synthesized compounds were confirmed by IR, NMR (^{1}H &^{13}C) and Mass spectral data. The presence of major IR signals for Succinamic acids were observed at 1672-1745 (Carbonyl groups), 2980-3100 (Aromatic –CH), 3145 (Acetamide) and 3250 (Carboxylic acids) νmax cm^{-1}. The ^{1}H -NMR spectrum of the succinamic acids showed two mutually coupled triplets for methylene at δ 2.2 to 2.7 (2H, t, CH_2, J = 6.9Hz), Aromatic protons at δ 6.5 to 7.8 as a doublet, acetamide (δ 8.76 (s, 1H) and carboxylic acids (δ 11.05 (s, 1H, D_2O exchangeable) groups. Further, the formation of final N-phenyl-4-oxo-butanamide derivatives was confirmed by the appearance of 2° amine protons accordingly and disappearance of carboxylic acid peak and is in agreement with absence of broad IR signal of it. Fig. 3 displays a

Table 1 — Substituent amines used in Scheme 1

Compd	R^1	Compd	R^1	R	
1a	Piperazine	**3a**	Piperazine	1	H
1b	1-Methyl Piperazine	**3b**	1-Methyl Piperazine	2	Cl
1c	1-Phenyl Piperazine	**3c**	1-Phenyl Piperazine	3	CH_3
1d	1-Benzyl Piperazine	**3d**	1-Benzyl Piperazine	4	2,4-difluoro
1e	Piperidine	**3e**	Piperidine	–	–
1f	Pyrrolidine	**3f**	Pyrrolidine	–	–
1g	Diethyl amine	**3g**	Diethyl amine	–	–
2a	Piperazine	**4a**	Piperazine	–	–
2b	1-Methyl Piperazine	**4b**	1-Methyl Piperazine	–	–
2c	1-Phenyl Piperazine	**4c**	1-Phenyl Piperazine	–	–
2d	1-Benzyl Piperazine	**4d**	1-Benzyl Piperazine	–	–
2e	Piperidine	**4e**	Piperidine	–	–
2f	Pyrrolidine	**4f**	Pyrrolidine	–	–
2g	Diethyl amine	**4g**	Diethyl amine	–	–

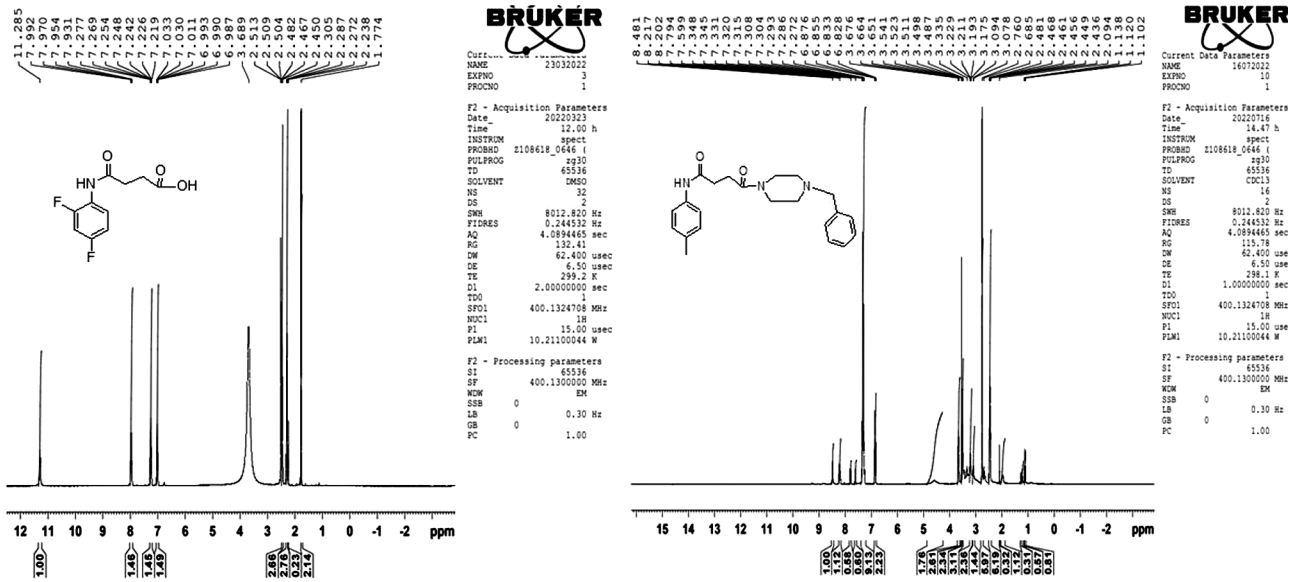

Fig. 3 — ^{1}H NMR spectra of Step 1 (Intermediate) and Step 2 (compound **4d**)

representative example of one of ^{1}H NMR spectra of succinamic acid and compound **4d**. The ^{13}C -NMR spectrum showed all the characteristic peaks according to the molecular structure, the most prominent carbon signals observed at δ 171.35 accounted for carbonyl peaks. The mass spectrum of all the compounds displayed their molecular ion peaks, which correspond to the M+1 peaks of the corresponding molecules and are consistent with their molecular formulas. The elemental/CHN analysis of the synthesized compounds yields satisfactory results.

The synthesized compounds **1a-g**, **2a-g**, **3a-g**, **4a-g** were subjected to *in vitro* MABA assay against *Mycobacterium tuberculosis* H37Rv to evaluate antitubercular activity wherein compounds **4c** and **4d**showed potent anti-TB activity with an MIC of 1.56 μg/mL given in Fig. 4 and Table 2. To assess their selectivity, the N-phenyl-4-oxo-butanamide derivatives were also tested for their antimicrobial activity. However, when tested at a concentration of 100 μg/mL, none of the synthesized compounds exhibited detectable antimicrobial activity against bacterial susceptibility.

To understand the binding mode of the N-phenyl-4-oxo-butanamide derivatives, all the synthesized compounds **1a-g**, **2a-g**, **3a-g**, **4a-g** were subjected to molecular docking studies against the five enzymes which are involved in mycolic acid biosynthesis pathway viz, 2-transenoyl-acyl carrier protein (ACP) reductase (5MTP), β-ketoacyl-ACP reductase (MabA), beta-ketoacyl-acyl carrier protein synthase III (1HZP), mycolic acid methyl transferase (MmaA1) and β-ketoacyl ACP synthase I (5LD8). The docking scores were predicted to be in the range of –7.4 to –

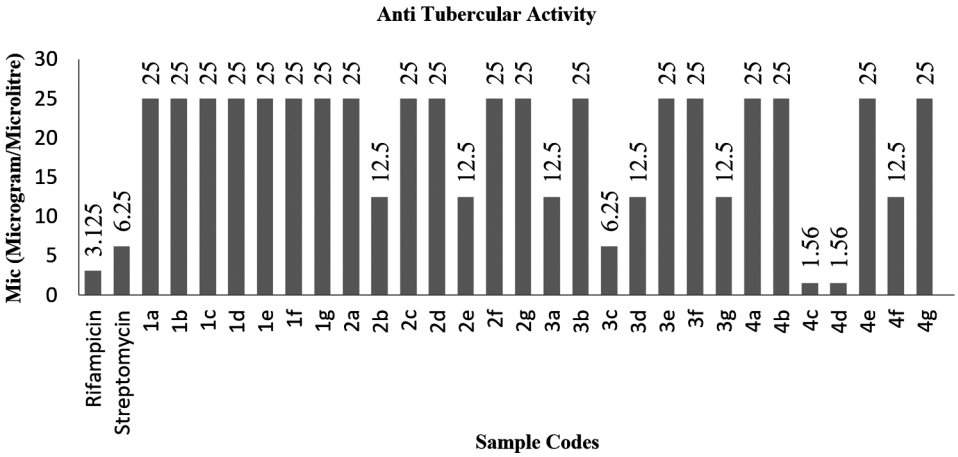

Fig. 4 — *In vitro* MABA assay results of the N-phenyl-4-oxo-butanamide derivatives **1a-g**, **2a-g**, **3a-g**, **4a-g**

Table 2 — Results of Antitubercular activity of N-phenyl-4-oxo-butanamide derivatives (MABA Assay)

S. No	Compd	MIC (μg/mL)	S. No	Compd	MIC (μg/mL)
1	**1a**	25	16	**3b**	25
2	**1b**	25	17	**3c**	6.25
3	**1c**	25	18	**3d**	12.5
4	**1d**	25	19	**3e**	25
5	**1e**	25	20	**3f**	25
6	**1f**	25	21	**3g**	12.5
7	**1g**	25	22	**4a**	25
8	**2a**	25	23	**4b**	25
9	**2b**	12.5	24	**4c**	1.56
10	**2c**	25	25	**4d**	1.56
11	**2d**	25	26	**4e**	25
12	**2e**	12.5	27	**4f**	12.5
13	**2f**	25	28	**4g**	25
14	**2g**	25	29	Streptomycin	6.25
15	**3a**	12.5	30	Rifampicin	3.125

10.6 kcal/mol. The N-phenyl-4-oxo-butanamide derivatives, particularly those substituted with phenyl and benzyl piperazine amines showed good binding affinity with all the five enzymes. Notably, derivatives (1c, 1d, 2c, 2d, 3c, 3d, 4c & 4d) were found to have very strong interactions with these amino acids Gly-14, Ser-20, Ala-22 and Gln-214 which are already reported to possess a sceptical role in the functioning of InhA, with docking scores ≥ 10.0 kcal/mol. Hence, the docking study further supports the activity profile observed in *in vitro* tests of the analogues. Fig. 5 and Table 3 represents the docking interactions of the most potent ligands (**4c** and **4d**) with the protein InhA.

Molinspiration is an online tool for predicting molecular physicochemical properties such as LogP, TPSA, Lipinski Rule of Five using a methodology that calculates drug transport properties as a sum of fragment based contributions and correction factors.[36-38] It was used to predict the physicochemical properties of the N-phenyl-4-oxo-butanamide derivatives. The topological polar surface area (TPSA) of the N-phenyl-4-oxo-butanamide derivatives was found to be between 49.41 and 61.43 A°, which is significantly lower than the 160 A° limit. The predicted percentage absorption for the N-phenyl-4-oxo-butanamide derivatives ranged from 87.80 to 91.95 percent, showing good oral bioavailability. Molinspiration was also used to predict the drug-likeness and bioactivity scores of the compounds. Based on bioactivity ratings, the compounds 1c, 1d, 3c, 3d, 4a, 4b, 4c, 4d, and 4f, were predicted as the most promising compounds.

The Osiris Property Explorer[39,40] is based on chemical artificial intelligence and chemoinformatics methods to predict the toxicity risks and drug scores for small molecules. The SMILES codes for the synthesized compounds were submitted to Osiris property explorer to predict the physicochemical and toxicological properties. In terms of mutagenicity, tumorigenicity, irritating impact, and reproductive effect, the results revealed that all the compounds were non-hazardous and likely to exhibit little or no toxicity.

Structural activity relationship studies:

The SAR of the N-phenyl-4-oxo-butanamide derivatives shows that the presence of halogens in

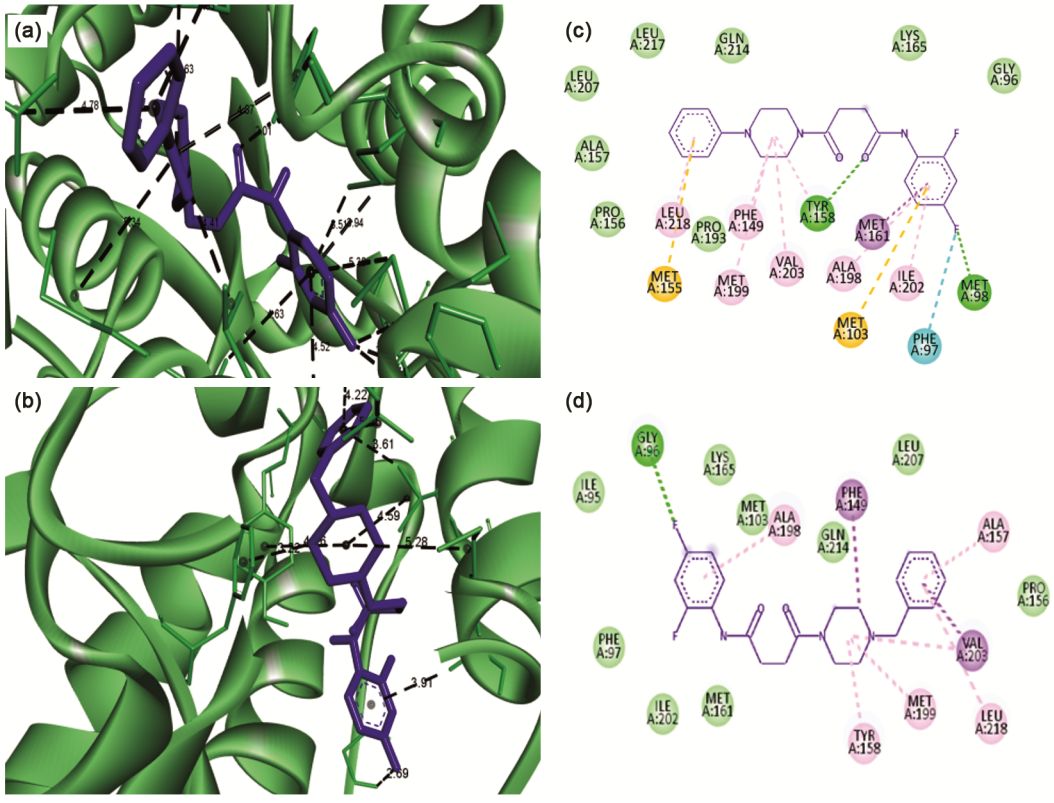

Fig. 5 — Docking poses of the potent molecules (**4c**, **4d**) with InhA enzyme. The protein was represented as green color solid ribbon model and the ligand as dark blue stick model. The 2D interaction diagram of the protein-ligand interaction is shown on the right side.

Table 3 — Molecular docking scores of N-phenyl-4-oxo-butanamide derivatives against enzyme (InhA)

S. No	Compd	Docking scores InhA (5MTP) kcal/mol	S. No	Compd	Docking scores InhA (5MTP) kcal/mol
1	**1a**	–7.7	15	**3a**	–8.5
2	**1b**	–8.1	16	**3b**	–8.6
3	**1c**	–10.0	17	**3c**	–10.2
4	**1d**	–9.9	18	**3d**	–10.3
5	**1e**	–8.5	19	**3e**	–9.1
6	**1f**	–8.1	20	**3f**	–8.5
7	**1g**	–7.4	21	**3g**	–7.9
8	**2a**	–8.3	22	**4a**	–8.6
9	**2b**	–8.6	23	**4b**	–8.5
10	**2c**	–10.0	24	**4c**	–10.6
11	**2d**	–10.0	25	**4d**	–10.4
12	**2e**	–8.8	26	**4e**	–8.5
13	**2f**	–8.3	27	**4f**	–8.5
14	**2g**	–7.8	28	**4g**	–7.4

aromatic amines increases bioactivity in the following order: 2, 4-di F > 4-Cl > CH3 (Fig. 6). On the other hand, the potency was significantly diminished by the presence of electron-donating groups on the aromatic ring. This signifies that the 1,4-dicarbonyl scaffold is essential for activity and further substitutions with N-substituted piperazine along with electron withdrawing groups aid in increasing its activity.

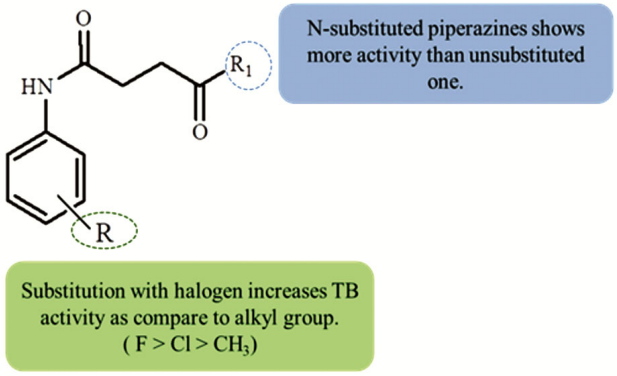

Fig. 6 — SAR Activity of N-phenyl-4-oxo-butanamide derivatives.

Conclusion

This new series of N-phenyl-4-oxo-butanamide derivatives obtained from molecular hybridisation were established as potential antitubercular compounds. Among all the derivatives, two compounds, **4c** (N-(2,4-difluorophenyl)-4-oxo-4-(4-phenylpiperazin-1-yl)butanamide) and **4d** (N-(2,4-difluorophenyl)-4-oxo-4-(4-benzylpiperazin-1-yl)butanamide), showed potent antitubercular activity against *M. tuberculosis* H37Rv with 1.56 µg/mL minimum inhibitory concentration (MIC), In specific, these compounds didn't show any noticeable antibacterial and antifungal activity in our studies. Molecular docking analysis of the test compounds showed good binding affinity with InhA when compared with other enzymes considered in the present study. SAR analysis signifies that the 1, 4-dicarbonyl scaffold is essential for activity and further substitutions with N-substituted piperazine along with electron withdrawing groups aid in increasing the activity of the compounds. *In silico* ADME analysis predicted that all the synthesized compounds show good bioactivity and very low toxicity risk. Therefore, the identified compounds can be putative leads for Tuberculosis drug discovery. Further research is required to enhance our understanding of the relationships between the structure and active site using a more extensive range of structurally related derivatives. Additionally, it is crucial to establish a correlation between the results of *in silico* docking studies to *in vitro* enzymatic experiments.

Acknowledgements

The authors thank the Director of the NMR Research Centre, Andhra University, Visakhapatnam, India, for providing the spectral data.

Supplementary Information

The manuscript is further supported by detailed Spectral characterization of all Compounds **1a-g**, **2a-g**, **3a-g**, **4a-g** data in the Supplementary Information. This includes physico-chemical properties,IR,

NMR (^{1}H and ^{13}C NMR), MS spectra, and CHNS analysis, followed by *in vitro* and *in silico* analysis results. Supplementary information is available in the website http://nopr.niscpr.res.in/handle/123456789/58776.

References

1 Fu L M & Fu-Liu C S, *Tuberculosis*, 82 (2002) 85.
2 Soolingen D V, Hoogenboezem T, Haas D P E, Hermans P W, Koedam M A, Teppema K S, Brennan P J, Besra G S, Portaels F, Top J & Schouls L M, *Int J Sys Evol Microbio*, 47 (1997) 1236.
3 Murray P R, Rosenthal K S & Pfaller M A, *Medical Microbiology E-book*, (Elsevier Health Sciences) 2020.
4 Van Ingen J, Rahim Z, Mulder A, Boeree MJ, Simeone R, Brosch R & Van Soolingen D, *Emerg Infec Dis*, 18 (2012) 653.
5 Rattan A, Kalia A & Ahmad N, *Emerg Infec Dis*, 4 (1998) 195.
6 Jackson M, McNeil M R & Brennan P J, *Fut Microbio*, 8 (2013) 855.
7 Heath R J, White S W & Rock C O, *Prog Lipid Res*, 40 (2001) 467.
8 Veyron-Churlet R, Molle V, Taylor R C, Brown A K, Besra G S, Zanella-Cléon I & Kremer L, *J Bio Chem*, 284 (2009) 6414.
9 Dessen A, Quémard A, Blanchard J S, Jacobs W R & Sacchettini J C,*Science*, 267 (1995) 1638.
10 Baldock C, Boer G J D, Rafferty J B, Stuitje A R & Rice D W, *Biochem Pharmacol*, 55 (1998) 1541.
11 Heath R J & Rock C O, *J Bio Chem*, 270 (1995) 26538.
12 Jackson M, McNeil M R & Brennan P J, *Future Microbio*, 8 (2013) 855.
13 Yuan Y, Crane D C, Musser J M, Sreevatsan S & Barry C E, *J Bio Chem*, 272 (1997) 10041.
14 Marrakchi H, Lanéelle M A & Daffe M, *Chem Bio*, 21 (2014) 67.
15 Zhang H J, Li L Z & Zhu L H, *Curr Med Chem*, 19 (2012) 1225.
16 Schaeffer M L, Agnihotri G, Volker C, Kallender H, Brennan P J & Lonsdale J, *J Bio Chem*, 276 (2001) 47029.
17 Marrakchi H, Lanéelle G & Quémard A, *Microbio*, 146 (2000) 289.
18 Turnowsky F, Fuchs K, Jeschek C & Högenauer G, *J bacteriology*, 171 (1989) 6555.
19 Veeravarapu H, Malkhed V, Mustyala K K, Vadija R, Malikanti R, Vuruputuri U, Muthyala M K, *Mol Diversity*, 25 (2021) 351.
20 Marrakchi H, Ducasse S, Labesse G, Montrozier H, Margeat E, Emorine L, Charpentier X, Daffé M & Quémard A, *Microbiology*, 148 (2002) 951.
21 Slayden R A, Lee R E & Barry C E, *Mol Microbio*, 38 (2000) 514.
22 Umarani W A, Sony K P, Hymavathi K V & Kumar M, *Indian J Chem*, 61 (2020) 411.
23 Veeravarapu H, Tirumalasetty M, Kurati S, Wunnava U & Muthyala M K, *Bioorg Med Chem Lett*, 30 (2020) 127603.
24 Ali M A, Moromi S K, Touchy A S & Shimizu K I, *Chem Cat Chem*, 8 (2016) 891.
25 Dhivare R S & Rajput S S, *World J Pharm Sci*, 4 (2015) 1650.
26 Vollhardt K P C, *Organic Chemistry*, (W H Freeman and Company, New York), 1987, pp 29-30.
27 Valeur E & Bradley M, *Chem Soc Rev*, 38 (2009) 606.
28 Palmino J C, Martin A, Camacho M, Guerra H, Swings J & Portales F, *Antimicro Agents Chemotherapy*, 46 (2002) 2720.
29 Franzblau S G, Witzig R S, McLaughlin J C, Torres P, Madico G, Hernandez A, Degnan M T, Cook M B, Quenzer V K, Ferguson R M & Gilman R H, *J Clinical Microbio*, 36 (1998) 362.
30 Collins L A & Franzblau S G, *Antimicro Agents Chemo*, 41 (1997) 1004.
31 Magaldi S, Mata-Essayag S, De Capriles C H, Pérez C, Colella MT, Olaizola C & Ontiveros Y, *Int J Infec Dis*, 8 (2004) 39.
32 Allinger N L, *J Ame Chem Soc*, 99 (1977) 8127.
33 Morris G M, Huey R, Lindstrom W, Sanner M F, Belew R K, Goodsell D S & Olson A J, *J Comp Chem*, , 30 (2009) 2785.
34 Trott O & Olson A J, *J Comp Chem*, 31 (2010) 455.
35 Accelrys Discovery Studio Visualiser, Version 3.5.
36 Ertl P, Rohde B & Selzer P, *J Med Chem*, 43 (2000) 3714.
37 Lipinski C A, Lombardo F, Dominy B W & Feeney P J, *Adv Drug Del Rev*, 64 (2012) 4.
38 Veber DF, Johnson SR, Cheng HY, Smith BR, Ward KW, Kopple KD, *J Med Chem*, , 45 (2002) 2615.
39 Sander T, Freyss J, Korff M V, Reich J R & Rufener C, *J Chem Info Mod*, 49 (2009) 232.
40 Hadda T B, Rastija V, Al-Malki F, Titi A, Touzani R, Mabkhot Y N, Khalid S, Zarrouk A & Siddiqui B S, *Curr Comp-Aided Drug Design*, 17 (2021) 123.